JOURNAL OF
biomaterials
applications

Biomaterials Processing

Journal of Biomaterials Applications
2018, Vol. 33(1) 94–102

DOI: 10.1177/0885328218771195
journals.sagepub.com/home/jba
SAGE

Influence of citric acid on the physical and biomineralization ability of freeze/thaw poly(vinyl alcohol) hydrogel

Mohamad Nizam Abdul Wahid[1], Saiful Izwan Abd Razak[1,2], Mohammed Rafiq Abdul Kadir[2], Rozita Hassan[3], Nadirul Hasraf Mat Nayan[4] and Khairul Anuar Mat Amin[5]

Abstract

This work reports the modification of freeze/thaw poly(vinyl alcohol) hydrogel using citric acid as the bioactive molecule for hydroxyapatite formation in simulated body fluid. Inclusion of 1.3 mM citric acid into the poly(vinyl alcohol) hydrogel showed that the mechanical strength, crystalline phase, functional groups and swelling ability were still intact. Adding citric acid at higher concentrations (1.8 and 2.3 mM), however, resulted in physically poor hydrogels. Presence of 1.3 mM of citric acid showed the growth of porous hydroxyapatite crystals on the poly(vinyl alcohol) surface just after one day of immersion in simulated body fluid. Meanwhile, a fully covered apatite layer on the poly(vinyl alcohol) surface plus the evidence of apatite forming within the hydrogel were observed after soaking for seven days. Gel strength of the soaked poly(vinyl alcohol)/citric acid-1.3 mM hydrogel revealed that the load resistance was enhanced compared to that of the neat poly(vinyl alcohol) hydrogel. This facile method of inducing rapid growth of hydroxyapatite on the hydrogel surface as well as within the hydrogel network can be useful for guided bone regenerative materials.

Keywords

Poly(vinyl alcohol), hydrogel, citric acid, biomimetic, simulated body fluid, hydroxyapatite

Introduction

Poly(vinyl alcohol) (PVA)-based hydrogels have been extensively explored and considered to be the most useful hydrogel as medical implant and bone tissue engineering materials due to their high water content and excellent compressive strength.[1,2] Since cartilage lacks vascularity and low mitotic ability of its chondrocytes,[3] a good contact with biocompatible and bioactive guided bone regenerative material is sought after.[4] In order to form hydrogels, PVA chains need to be crosslinked for it to swell in the presence of water or biological fluid. Crosslinking can be done in several ways including physical,[5] chemical[6] or high-energy radiation.[7] Physical crosslinking of the PVA using repeated cycles of freezing and thawing can be the most preferred approach since it is feasible, cost savvy and eliminates the use of harmful chemical crosslinking agents. The hydrogel network is created through the crosslinking sites of the aggregation of micro crystals upon the freeze–thaw treatment. Although being useful in certain applications, hydroxyl groups of the PVA is not sufficient for obtaining good contact with bone tissue and lacks the ability of promoting bone growth.[8] Biologically active apatite layer

[1]Centre for Advanced Composite Materials, Universiti Teknologi Malaysia, Skudai, Johor, Malaysia
[2]Medical Devices and Technology Group, Faculty of Biosciences and Medical Engineering, Universiti Teknologi Malaysia, Skudai, Johor, Malaysia
[3]Orthodontic Unit, School of Dental Science, Universiti Sains Malaysia, Kubang Kerian, Kelantan, Malaysia
[4]Faculty of Engineering Technology, Universiti Tun Hussein Onn, Batu Pahat, Johor, Malaysia
[5]School of Fundamental Science, Universiti Malaysia Terengganu, Kuala Terengganu, Terengganu, Malaysia

Corresponding author:
Saiful Izwan Abd Razak, Faculty of Biosciences and Medical Engineering, Centre for Advanced Composite Materials, Universiti Teknologi Malaysia, Building V01, Skudai 81300, Malaysia.
Email: saifulizwan@utm.my

should be developed on the surface of the hydrogels for bonding with living bone.

Several methods demonstrated enhanced bioactivity of the PVA hydrogels which includes adding synthetic hydroxyapatite (HA) particles,[9–11] nanoclays[12] and bioactive glass.[13] Since the mixing approach utilizes components that form hybrids or composite hydrogel, a more viable and cost-effective method to promote bioactivity should be explored. Citric acid (CA) is a small organic acid molecule that has been widely used in the food and pharmaceutical industries[14] and it exists in its citrate form in fresh wet bone.[15] Several studies have demonstrated that the CA positively influenced the growth of HA on various substrates immersed in simulated body fluid (SBF) such as chitosan,[16] cellulose,[17] lignocellulosic fibres,[18] elastin-like recombinamers[19] and collagen membrane.[20] Furthermore, it was described that the inclusion of CA during the preparation of sol–gel HA resulted in high bioactivity in SBF.[21] Conversely, it was reported that addition of CA above 2 mM on collagen surface inhibits the formation of HA.[20]

Therefore, we hypothesized that physical crosslinking of PVA with the presence of CA could improve the osteogenic potential of the hydrogel. Thus, the aim of this study is to develop PVA/CA hydrogels with intact physical properties and enhanced biomineralization ability.

Experimental

Preparation of PVA/CA hydrogels

CA was purchased from Sigma-Aldrich and used without further purification. Required concentrations of CA containing freeze–thaw solutions (0.15, 0.8, 1.3, 1.8 and 2.3 mM) were prepared by dissolving solid CA in deionized (DI) water. PVA powder (Sigma-Aldrich, molecular weigth [Mw] = 89,000–98,000) with 15% by weight (wt%) was gradually added into the CA solution at a temperature of 90°C with a continuous mechanical stirring for 1 h. The PVA solution was then poured into a cylindrical acrylic mould with a height of 20 mm and a diameter of 15 mm and treated to freezing at −20°C for 24 h and followed by thawing at 23°C for 24 h. Three cycles were conducted at constant humidity. Following this procedure, PVA/CA hydrogels with various CA concentrations were prepared. Schematic preparation of the PVA/CA hydrogels is depicted in Figure 1.

Characterizations

Gel strength. A mechanical tester (Brookfield Engineering Laboratories) was used to measure the compressive gel strength (wet state) with downward probing rate of 0.5 mm/s until the sample reached the base. The cylindrical dimensions of the hydrogels were 20 mm (height) and 15 mm (diameter) according to the mould size. Five replications were done.

Fourier transform infrared. Fourier transform infrared (FTIR) vibrational spectra were obtained using a spectrometer, Nicolet iS5, with spectral resolution of 4 cm^{-1} averaging 16 scans in the scanning range of 600–4000 cm^{-1}.

X-ray diffraction. X-ray diffraction (XRD) diffractograms were collected using Siemens Model D500 diffractometer using CuKα radiation ($\lambda = 0.154$ nm),

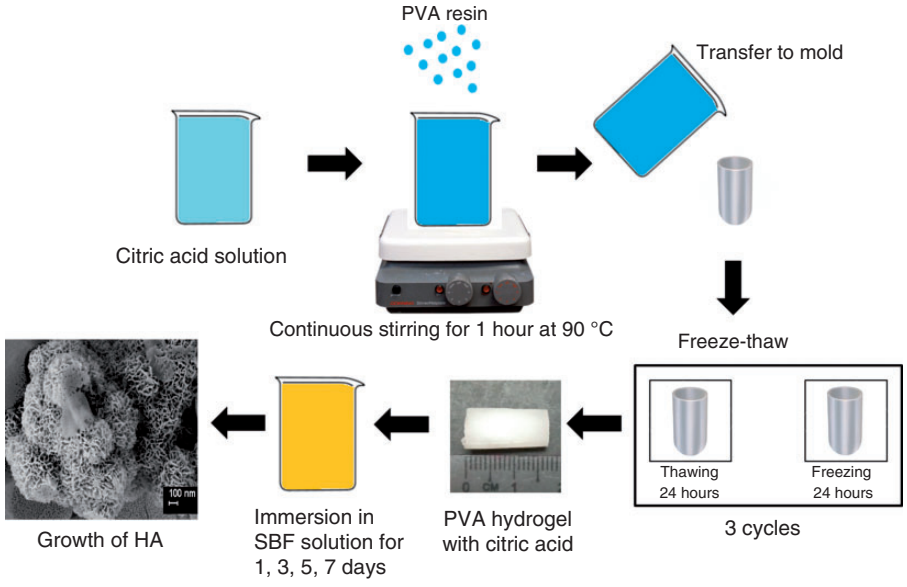

Figure 1. Schematic preparation of PVA/CA hydrogels.

employing scanning rate of 0.02 s^{-1} in the 2θ range from 5° to 90°.

Water contact angle. Water contact angle was measured and the image was captured using VCA Optima, AST Products. At least five replications were conducted for each sample.

Swelling. Equilibrium swelling in SBF and DI water were calculated as $(W_h - W_d)/W_h \times 100\%$ where W_h and W_d were the weights of the samples in the swollen state and dried state, respectively. Five replications were tested for each sample.

Morphology. Surface morphology of the hydrogels was investigated using scanning electron microscope (SEM, Leo Supra 50VP) equipped with an energy dispersive X-ray (EDX) system. To observe the internal surface of the hydrogel, selected sample was immersed in dry ice for 1 h and then fractured transversely.

Statistical analysis. The error bars on each point of the graphs correspond to the standard deviation of the mean.

In vitro biomineralization

In vitro biomineralization of the hydrogel was conducted by immersion in SBF solution. Preparation of the mimicking solution has been reported in detail elsewhere.[22,23] The ionic compositions and concentrations of the prepared SBF were similar to human blood plasma. Briefly, the solution was prepared by dissolving reagent-grade $CaCl_2$, NaCl, KCl, $MgCl_2{\cdot}6H_2O$, $K_2HPO_3{\cdot}3H_2O$, $NaHCO_3$ and Na_2SO_4 in ion-exchanged distilled water and buffering to pH 7.4 with tris-(hydroxymethyl)-aminomethane and HCl. The hydrogel was immersed in 25 mL of the prepared SBF solution and placed in an incubator at 36.5°C for 1, 3, 5 and 7 days. Then the samples were subjected to SEM, Ca/P ratio analysis by EDX, FTIR and gel strength in order to evaluate the effects of soaking in SBF.

Results and discussion

Gel strength

Effects of various CA concentrations on the gel strength of the PVA hydrogel are shown in Figure 2. Neat PVA hydrogel revealed gel strength of typically prepared freeze–thawed hydrogel. The gel strength was stable with the inclusion of CA up to 1.3 mM. This signifies that the gelation and forming of semi-crystalline phase during the freeze–thawing process was not interrupted with the presence of CA. Physical crosslinking of the PVA chains can be regarded as the main factor that gives the PVA its gel-like behaviour. In this case, the presence of CA at concentrations of 0.15–1.3 mM did not influence the mechanical response of the PVA hydrogel. Significant reduction was observed as the concentration reached 1.8 mM and was followed by 40% drop for the PVA/CA-2.3 mM sample. The presence of citrate ions at these concentrations might inhibit the formation of crystalline junctions due to the taking up of the CA forming H bond with the PVA chain. Thus, the loading capacity of the PVA hydrogel during the compressive stress reduced as a result of poor formation of crystalline junctions.

FTIR spectroscopy

Figure 3(a) depicts the FTIR spectrum of neat freeze–thawed PVA hydrogel. The spectrum displayed characteristic peaks that of PVA. Peaks at 3306 and 1644 cm^{-1} represent the O–H stretching and deformation vibrations, respectively. Peaks at 2945, 1417 and 1328 cm^{-1} correspond to the C–H stretching, C–H bond and C–C stretching, respectively. Peak at 1090 cm^{-1} represent C–O stretching vibration. The most significant vibration for PVA in its hydrogel form is the C–C–C bond

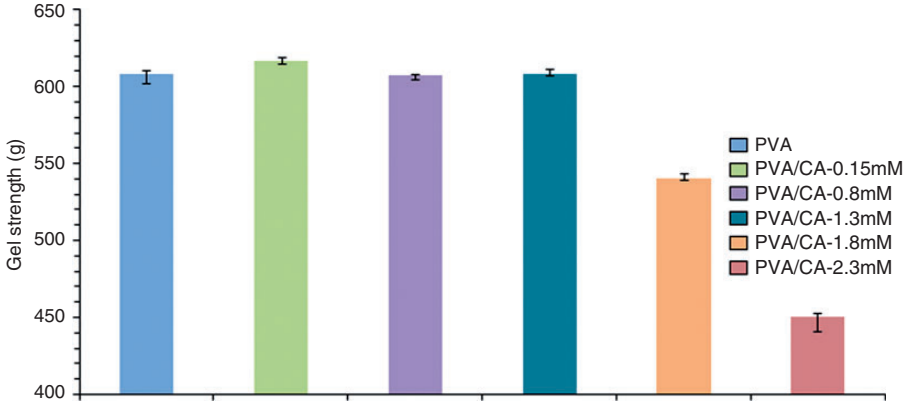

Figure 2. Gel strength of neat PVA hydrogel and PVA hydrogels with CA inclusions.

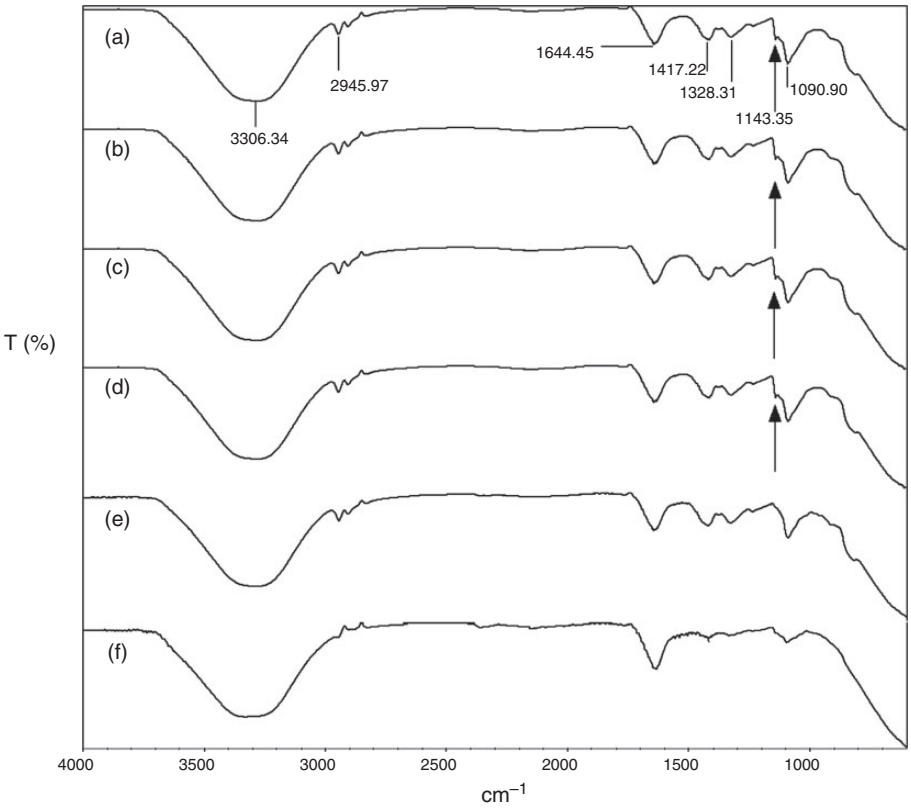

Figure 3. FTIR spectra of (a) neat PVA, (b) PVA/CA-0.15 mM, (c) PVA/CA-0.8 mM, (d) PVA/CA-1.3 mM, (e) PVA/CA-1.8 mM and (f) PVA/CA-2.3 mM.

stretching vibration at 1143 cm^{-1}. This vibration corresponds to the crystalline domains of the PVA hydrogel.[24] Spectra of PVA hydrogels at CA concentrations of 0.15, 0.8 and 1.3 mM (Figure 3(b) to (d)) revealed similar vibrational peaks to that of neat PVA. Based on the spectrum analysis, the CA did not induce any covalent bonding or chemical reaction with the PVA. In addition, the presence of the 1143 cm^{-1} peak signifies that the crystalline domain of PVA still exists. Samples of PVA/CA-1.8 mM and PVA/CA-2.3 mM detected no 1143 cm^{-1} peak vibration. This was due to the poor formation of physical crosslink junction which corroborates the gel strength findings.

X-ray diffraction

XRD spectrum of the neat PVA hydrogel (Figure 4(a)) displayed the characteristic diffraction plane (101) of PVA hydrogel at 20° which represent the semi-crystalline nature of PVA.[25] PVA hydrogels with 0.15, 0.8 and 1.3 mM CA (Figure 4(b) to (d)) showed no new diffraction peaks and the 20° peak intensity remains unchanged. This indicates that the CA did not create any new phases in the hydrogel and the crystalline domain of the PVA is still intact. It can be suggested that the CA form interactions with the available PVA chains without disrupting the crystalline domain of the PVA. Peak intensity (101) for the 1.8 and 2.3 mM samples (Figure 4(e) and (f)) reduced considerably compared to that of neat PVA.

Water contact angle (WCA) and swelling

WCA is an effective method to measure hydrophilicity of the hydrogels. Table 1 shows that the WCA of the 0.15, 0.8 and 1.3 mM PVA/CA samples reduced as compared to that of neat PVA. Its corresponding images depict the spreading of the water droplet on the surface. CA provides additional water adhering capacity to the hydrogel surface through its polar OH groups thus obtaining minor contact angle. In case of biomineralization, hydrophilic surface is preferable for bonding between the PVA substrate and surrounding SBF ions. For the 1.8 and 2.3 mM PVA/CA samples, the contact angle was substantially lowered to $14.0 \pm 0.98°$ and $12.5 \pm 0.43°$, respectively. This can be explained by the increased amount of available OH groups of PVA that did not participate in the formation of crystalline junctions. Equilibrium swelling of the hydrogel samples in DI water and SBF are included in Table 1. All the hydrogel samples showed lower swelling in SBF compared to that of DI water due to the decreased osmotic

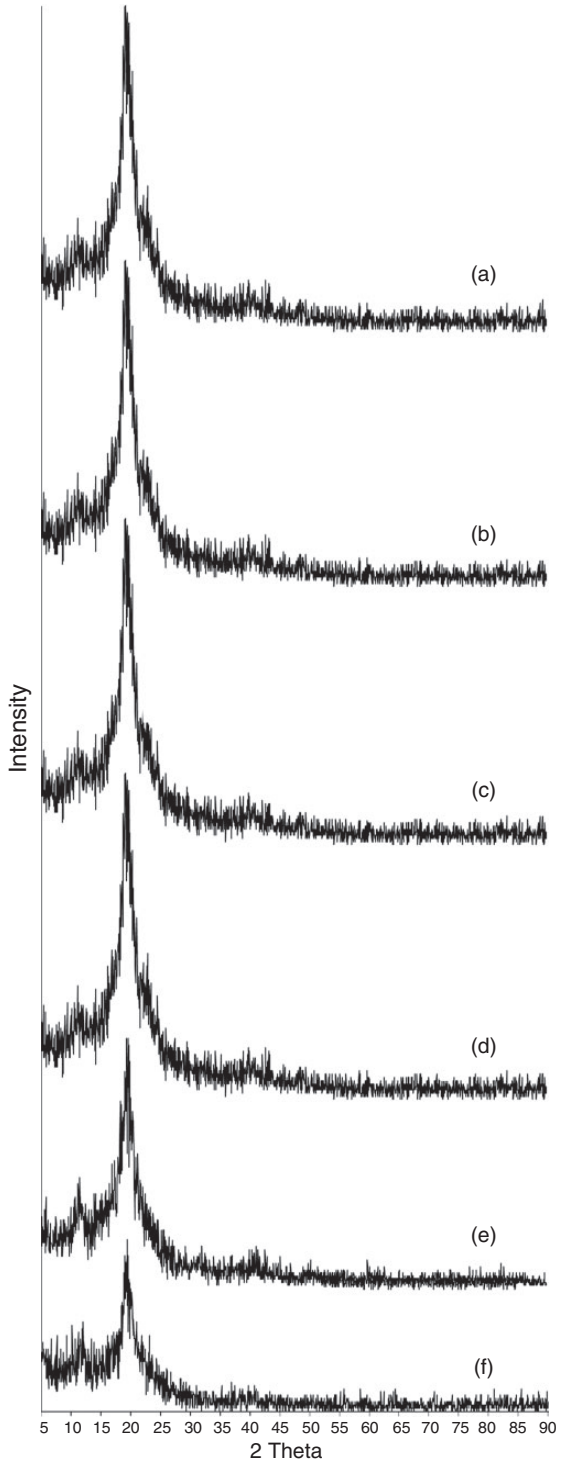

Figure 4. XRD spectra of (a) neat PVA, (b) PVA/CA-0.15 mM, (c) PVA/CA-0.8 mM, (d) PVA/CA-1.3 mM (e) PVA/CA-1.8 mM and (f) PVA/CA-2.3 mM.

pressure of water surrounded by the SBF ions. The CA at low concentrations (0.15, 0.8 and 1.3 mM) did not significantly influence the swelling behaviour of the PVA hydrogels, both in DI water and SBF. Meanwhile, increased in swelling in DI water and SBF were observed for the 1.8 and 2.3 mM PVA/CA samples. This was due to the expansion of PVA chains that interacts with the abundantly available CA ions.

It was established that CA at concentrations of 0.15, 0.8 and 1.3 mM can be incorporated within the PVA to form mechanically stable hydrogel with intact functional groups and crystalline phase, surface hydrophilicity and excellent swelling characteristics. Since the aim of CA in the PVA hydrogel is to provide biofunctionality towards the formation of HA in vitro, higher concentration of CA with no detrimental effects towards the PVA hydrogel can be suggested. Thus, PVA/CA-1.3 mM hydrogel was selected for the in vitro biomineralization in SBF. Although higher swelling capability and reduced contact angle was obtained for the 1.8 and 2.3 mM PVA/CA hydrogels, their physical response was poor.

In vitro biomineralization

SEM image of Figure 5(a) depict the morphology of PVA hydrogel without addition of CA after seven days of soaking in SBF. The presence of pores may due to the infiltration and ion exchange between water and the SBF ions. This morphology could be useful conditions for transferring of nutrients, lubricants, tissue fluid and for clinical reconstructive material. Furthermore, no obvious apatite mineralization was observed on the surface. The OH groups of PVA are considered to be non-bioactive in terms of HA growing capability due to lack of net charge. It was reported that PVA hydrogels prepared by sol–gel method needed pre-embedded apatite particles in order to grow the HA in SBF, it takes up to seven days to do so.[26]

Addition of 1.3 mM CA in the PVA hydrogel promotes the growth of HA after one day of soaking in SBF. Few HA particles were formed on the surface. Figure 5(b) displayed SEM image of the HA spherulites having porous spheroidal structure. The HA formation can be elucidated by the presence of CA in the PVA hydrogel. CA consists of three COOH groups and one OH group that ionize into citrate ion in SBF. The OH groups of CA can form H bonds with OH groups of PVA, while the COO^- can chelate with the calcium ions of SBF forming complex. The process then continues by attracting phosphate ions, other calcium ions and other citrate ions on the chelate complex that lead to the nucleation of HA crystals. Figure 6 illustrates the proposed biomimetic mineralization of the HA assisted by the CA component. SEM images of Figure 5(c) to (e) showed the evolution of apatite on the PVA surface after soaking in SBF for three, five and seven days, respectively. A fully covered apatite layer can be observed after three days of soaking in SBF followed by fusing of HA crystals as the soaking time increased

Table 1. Water contact angle and degree of swelling of neat PVA hydrogels.

	Water contact angle		Degree of swelling (%)	
Sample	Value (°)	Image	DI water	SBF
PVA	25.5 ± 0.42		314.7 ± 2.2	283.6 ± 1.8
PVA/CA-0.15 mM	19.8 ± 0.78		315.8 ± 1.9	284.1 ± 3.4
PVA/CA-0.8 mM	19.0 ± 0.12		314.6 ± 4.8	282.8 ± 7.8
PVA/CA-1.3 mM	18.9 ± 0.66		315.3 ± 2.5	286.2 ± 3.2
PVA/CA-1.8 mM	14.0 ± 0.98		356.7 ± 6.8	297.3 ± 7.3
PVA/CA-2.3 mM	12.5 ± 0.43		384.4 ± 5.4	320.5 ± 4.6

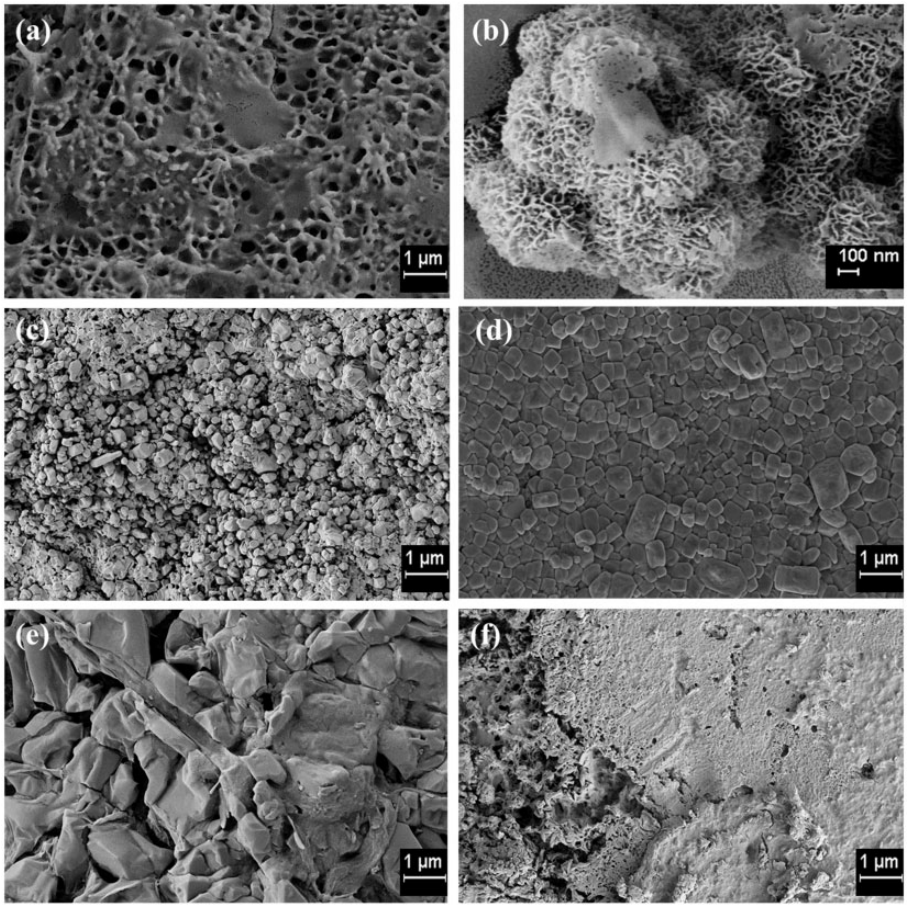

Figure 5. SEM micrographs of (a) neat PVA soaked for seven days, (b) PVA/CA-1.3 mM soaked for one day, (c) PVA/CA-1.3 mM soaked for three days, (d) PVA/CA-1.3 mM soaked for five days, (e) PVA/CA-1.3 mM soaked for seven days and (f) cross-sectional of PVA/CA-1.3 mM soaked for seven days.

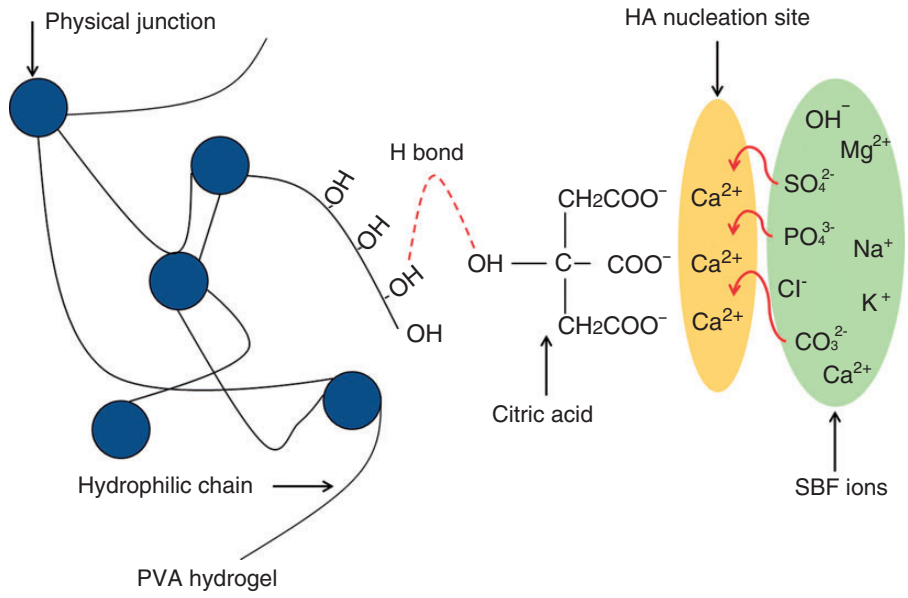

Figure 6. Proposed surface interactions and biomineralization process.

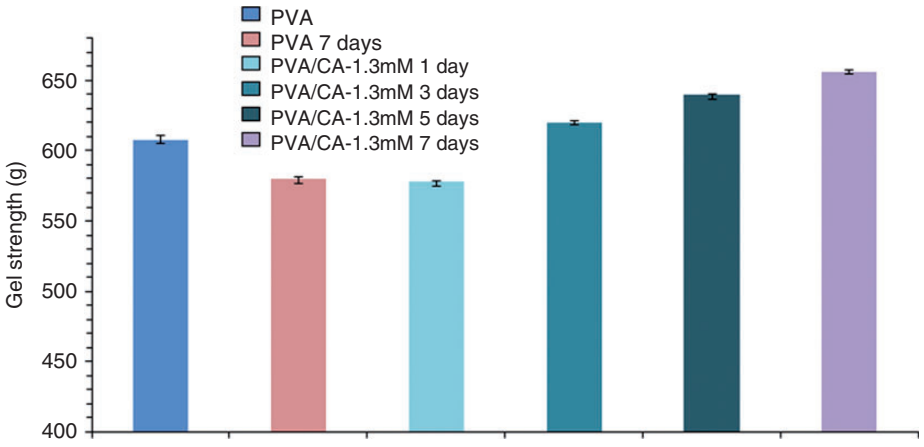

Figure 7. Gel strength of PVA hydrogels after soaking in SBF.

up to seven days. The Ca/P ratio obtained was 1.95 $\pm$ 0.76, 1.83 $\pm$ 0.20, 1.74 $\pm$ 0.17, 1.65 $\pm$ 0.08 for samples soaked in SBF for period of one, three, five and seven days, respectively. Progressive reduction of the Ca/P ratio was due to the precipitation of a nonstoichiometric calcium-deficient HA from SBF.

Although the apatite formation on the PVA surfaces is evident, the inner part of the hydrogel should be investigated as well. Figure 5(f) revealed that the apatite was also formed inside the PVA/CA-1.3 mM sample soaked for seven days. The freeze–thaw CA solution provides nucleating effects within the PVA hydrogel. Swelling of the PVA hydrogel opens up spaces for the growth of HA crystals. Ca/P ratio of the inner HA was quite similar to its outer surface grown HA (1.67 $\pm$ 0.13) which implies that the CA can provide bioactivity within the PVA hydrogel. Thus, cell culture studies in near future would provide further insights for cartilage repair and guided bone regeneration material applications.

Figure 7 describes gel strength of the hydrogels after being soaked in SBF. Neat PVA soaked in SBF for seven days showed lower gel strength compared to its un-soaked counterpart. This was due to the infiltration of the SBF ions that lead to the opening up of PVA domain. PVA/CA-1.3 mM soaked for one day, however, did not show any mechanical changes compared to the neat PVA soaked for seven days. It can be proposed that no HA was formed within the hydrogel sample after soaking in SBF for one day. Interestingly, gel

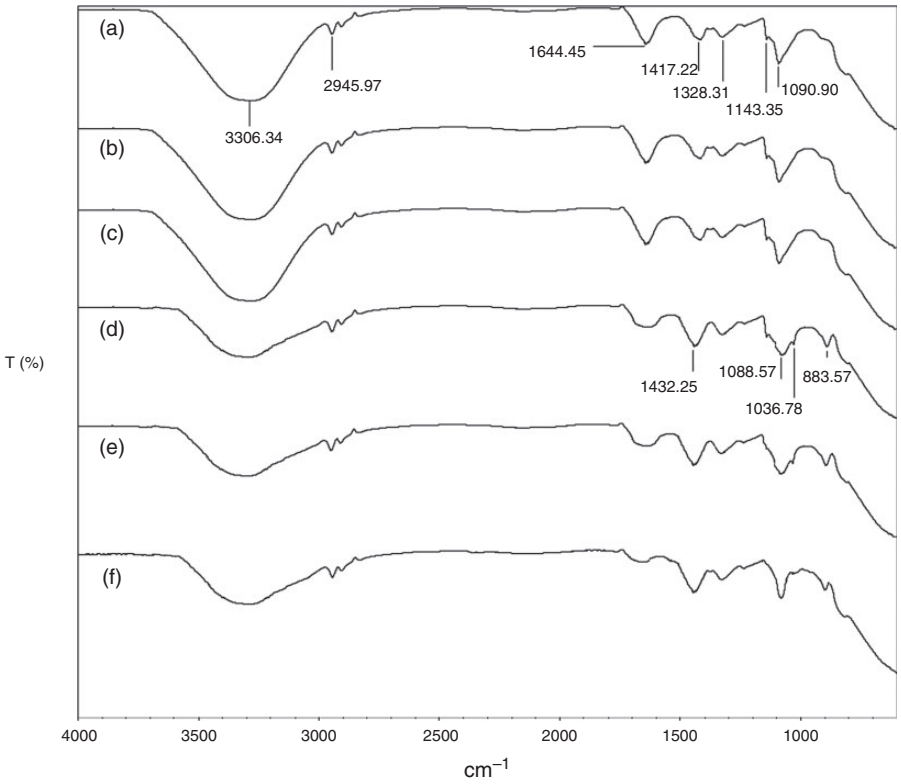

Figure 8. FTIR spectra of (a) un-soaked neat PVA, (b) soaked neat PVA for seven days, (c) PVA/CA-1.3 mM soaked for one day, (d) PVA/CA-1.3 mM soaked for three days, (e) PVA/CA-1.3 mM soaked for five days and (f) PVA/CA-1.3 mM soaked for seven days.

strength of the PVA increased with increasing soaking time starting from three days up to seven days of soaking. The HA component which grown inside the PVA provides additional strength to the hydrogel by filling up the pores thus making the hydrogel more tolerant to withstand extra load. The increment also suggest that more HA crystals formed within the hydrogel as the soaking time increased. The biomimetic growth of HA within the PVA hydrogel could provide useful load-bearing capability for cartilage, and thus a good bonding with the implantation site.

FTIR spectrum of the neat PVA hydrogel soaked in SBF for seven days (Figure 8(b)) showed similar pattern to that of un-soaked PVA hydrogel (Figure 8(a)). Similar pattern was also observed for the PVA/CA-1.3 mM soaked in SBF for one day (Figure 8(c)). In both cases (neat PVA with seven days of soaking and PVA/CA-1.3 mM with one day of soaking), no HA-related peaks was observed. Although the previous SEM image (Figure 5(b)) showed the presence of HA, detection of the component is difficult since only few HA crystals are present. PVA/CA-1.3 mM samples with soaking time of three, five and seven days (Figure 8 (d) to (f)) on the other hand showed the emergence of phosphate ion stretching modes at 1088 and 1036 cm^{-1} and carbonate ion out-of-plane stretching mode at 1432 and 883 cm^{-1}. Furthermore, reduction of the OH-related vibrations (3306 and 1644 cm^{-1}) signifies that the hydrogel surface is dominated by the apatite.

Conclusions

It was shown that the addition of CA concentration of 0.15, 0.8 and 1.3 mM did not affect properties of the resulting freeze–thawed PVA hydrogel. The gel strength, functional groups, crystalline phase, swelling and water contact angle of the modified PVA hydrogels were displayed to be physically useful biomedical applications. When the CA concentration was increased to 1.8 and 2.3 mM, detrimental impacts were observed. CA inclusion was shown to be useful for the growing of HA on the less bioactive PVA. In vitro biomineralization of the PVA/CA-1.3 mM sample revealed the formation of HA crystals on the surface and internal of the hydrogel. The nucleation mechanism of HA could be clarified by the attachment of the CA onto the hydrophobic PVA and simultaneously forming chelate complex that provides sites for the growth of HA nuclei. Immersion of the PVA/CA-1.3 mM sample in SBF revealed that the gel strength increased with increasing the soaking time. Substantial filling up of the hydrogel spaces by HA component that lead to

high compressive strength can be suggested. This new approach of inducing bioactivity to the PVA hydrogel has prospective for guided bone regeneration due to the rapid apatite growth on the surface and within the hydrogel. Furthermore, simple approach of adding CA into freeze–thawed hydrogel might facilitate the fabricating and manufacturing of biomedical materials.

Declaration of Conflicting Interests

The author(s) declared no potential conflicts of interest with respect to the research, authorship, and/or publication of this article.

Funding

The author(s) received no financial support for the research, authorship, and/or publication of this article.

ORCID iD

Saiful Izwan Abd Razak http://orcid.org/0000-0001-7477-0284

References

1. Gaaz TS, Kadhum AAH, Michael PKA, et al. Unique halloysite nanotubes–polyvinyl alcohol–polyvinylpyrrolidone composite complemented with physico–chemical characterization. *Polymers* 2017; 9: 207.
2. Lin HY, Tsai WC and Chang SH. Collagen-PVA aligned nanofiber on collagen sponge as bi-layered scaffold for surface cartilage repair. *J Biomater Sci Polym Ed* 2017; 28: 664–678.
3. Park H, Lee HJ, An H, et al. Alginate hydrogels modified with low molecular weight hyaluronate for cartilage regeneration. *Carbohydr Polym* 2017; 162: 100–107.
4. Cao L, Zhang F, Wang Q, et al. Fabrication of chitosan/graphene oxide polymer nanofiber and its biocompatibility for cartilage tissue engineering. *Mat Sci Eng C Mater* 2017; 79: 697–701.
5. Hong KH. Polyvinyl alcohol/tannic acid hydrogel prepared by a freeze-thawing process for wound dressing applications. *Polym Bull* 2017; 74: 2861–2872.
6. Gao Z, Yu Z, Huang C, et al. Carboxymethyl cellulose reinforced poly (vinyl alcohol) with trimethylol melamine as a chemical crosslinker. *J Appl Polym Sci* 2017; 134: 44590.
7. Entezam M, Daneshian H, Nasirizadeh N, et al. Hybrid hydrogels based on poly (vinyl alcohol)(PVA)/agar/poly (ethylene glycol)(PEG) prepared by high energy electron beam irradiation: Investigation of physico-chemical and rheological properties. *Macromol Mater Eng* 2017; 302: 1600397.
8. Zheng Y, Lv H, Wang Y, et al. Performance of novel bioactive hybrid hydrogels in vitro and in vivo used for artificial cartilage. *Biomed Mater* 2009; 4: 015015.
9. Chen K, Liu J, Yang X, et al. Preparation, optimization and property of PVA-HA/PAA composite hydrogel. *Mat Sci Eng C Mater* 2017; 78: 520–529.
10. Zheng Y, Wang YJ, Chen X, et al. Preparation and characterization of poly (vinyl alcohol)/hydroxylapatite hybrid hydrogels. *J Compos Mater* 2007; 41: 2071–2082.
11. Yusong P, Dangsheng X and Xiaolin C. Mechanical properties of nanohydroxyapatite reinforced poly (vinyl alcohol) gel composites as biomaterial. *J Mater Sci* 2007; 42: 5129–5134.
12. Azmi S, Razak SIA, Abdul Kadir MR, et al. Reinforcement of poly (vinyl alcohol) hydrogel with halloysite nanotubes as potential biomedical materials. *Soft Mater* 2017; 15: 45–54.
13. Tang Y, Pang L and Wang D. Preparation and characterization of borate bioactive glass cross-linked PVA hydrogel. *J Non-Cryst Solids* 2017; 476: 25–29.
14. Ciriminna R, Meneguzzo F, Delisi R, et al. Citric acid: emerging applications of key biotechnology industrial product. *Chem Cent J* 2017; 11: 22.
15. Hartles RL. Citrate in mineralized tissues. *Adv Oral Biol* 1963; 1: 225–253.
16. Liu Y, Shen X, Zhou H, et al. Chemical modification of chitosan film via surface grafting of citric acid molecular to promote the biomineralization. *Appl Surf Sci* 2016; 370: 270–278.
17. Hong L, Wang YL, Jia SR, et al. Hydroxyapatite/bacterial cellulose composites synthesized via a biomimetic route. *Mater Lett* 2006; 60: 1710–1713.
18. Razak SIA, Wahab IF, Kadir MR, et al. Biomimetic growth of hydroxyapatite on kenaf fibers. *BioResources* 2016; 11: 1971–1981.
19. Sánchez-Ferrero A, Mata Á, Mateos-Timoneda MA, et al. Development of tailored and self-mineralizing citric acid-crosslinked hydrogels for in situ bone regeneration. *Biomaterials* 2015; 68: 42–53.
20. Rhee SH and Tanaka J. Effect of citric acid on the nucleation of hydroxyapatite in a simulated body fluid. *Biomaterials* 1999; 20: 2155–2160.
21. Kaygili O, Keser S, Kom M, et al. The effect of simulating body fluid on the structural properties of hydroxyapatite synthesized in the presence of citric acid. *Prog Biomater* 2016; 5: 173–182.
22. Wang M, Li Y, Wu J, et al. In vitro and in vivo study to the biocompatibility and biodegradation of hydroxyapatite/poly (vinyl alcohol)/gelatin composite. *J Biomed Mater Res A* 2008; 85: 418–426.
23. Kokubo T and Takadama H. How useful is SBF in predicting in vivo bone bioactivity? *Biomaterials* 2006; 27: 2907–2915.
24. Wei W, Song W and Zhang S. Preparation and characterization of hydroxyapatite-poly (vinyl alcohol) composites reinforced with cellulose nanocrystals. *BioResources* 2014; 9: 6087–6099.
25. Karimi A, Daud W and Ashri WM. Harmless hydrogels based on PVA/Na+-MMT nanocomposites for biomedical applications: fabrication and characterization. *Polym Compos* 2015; 38: 1135–1143.
26. Zheng YD, Wang YJ, Chen XF, et al. Bioactive hydroxyapatite/polyvinyl alcohol composite for repair and regeneration of articular cartilage. *Key Eng Mater* 2007; 330: 475–478.